PAPER Nr.:34

AERODYNAMIC LOADS ON AN UNSTEADY AEROFOIL WITH A DEFLECTING TAB

BY

J.P. NARKIEWICZ, A.LING, G.T.S. DONE

CITY UNIVERSITY, LONDON, UK

TWENTIETH EUROPEAN ROTORCRAFT FORUM
OCTOBER 4 - 7, 1994 AMSTERDAM

Printed by the Technical Highschool Haarlem

Twentieth European Rotorcraft Forum
Amsterdam, The Netherlands, October 1994

Aerodynamic Loads on an Unsteady Aerofoil with a Deflecting Tab

J.P. Narkiewicz[1], A. Ling[2], G.T.S. Done
City University, London, UK

Abstract

A thin, low cambered aerofoil with a tab at the trailing edge in incompressible, unstalled flow is considered. The general expressions for unsteady lift and aerodynamic moment on aerofoil and tab are derived using two dimensional potential theory extended for the case of varying free stream velocity and arbitrary, different motions for both aerofoil and tab. To complete the method the lift deficiency function should be calculated for a particular wake shape and its time dependence.

To validate this approach, the classical Theodorsen case of an oscillating aerofoil is presented. Loads are calculated in the time domain by applying inverse Laplace transformation to the approximation of the lift deficiency function in the frequency domain. The agreement of the results calculated by this method with the results obtained by other methods and experiments is good.

The aerodynamic loads for the case of arbitrary motions of aerofoil and tab are also investigated.

Notation.

ab - distance of aerodynamic centre from aerofoil midchord
b - half of aerofoil chord
bc_t - the distance of tab hinge from midchord
$C(t,\gamma_w)$ - lift deficiency function
C_L - lift coefficient
C_M - moment coefficient
k - reduced frequency, k= wb/U
L(t) - lift
M(t) - moment
Ma - Mach number of undisturbed flow
p(t,x) - pressure distribution
Q(t) - velocity component in circulatory part
s - variable in Laplace transformation $s=i\omega t$
t - time,
x - coordinate along aerofoil chord
U(t) - free stream velocity
U_0 - relative free steam velocity
w(t) - aerofoil velocity component perpendicular to the chord
W(x,t) - flow velocity component perpendicular to the chord
$\alpha(t)$ - aerofoil angle of incidence
$\gamma(x,t)$ - distribution of circulation
$\delta(t)$ - angle of tab deflection
θ - spatial variable $\cos\theta = x/b$
$\lambda(x,t)$ - velocity component induced by circulation
ρ - air density,
$\varphi(x,t)$ - velocity potential
ϕo - angular coordinate of tab hinge
ζ - wake coordinate along x axis

Indexes
(α) - calculated for aerofoil without tab
(b) - calculated for aerofoil/tab
(t) - calculated for tab only
(w) - calculated for wake,
( ) - differentiation with respect to time
(C) - circulatory part
(N) - noncirculatory part

---

[1]On sabbatical from Warsaw University of Technology, Warsaw, Poland

[2] On sabbatical from the Chinese Helicopter Research and Development Institute, Jingdezhen, Peoples Republic of China

1. Introduction.

Calculation of aerodynamic loads is a crucial part of aeroelastic analysis of fixed and rotary wing aircraft. Despite the latest achievements in Computational Fluid Dynamics, the capability of solving full equations of flow around an aerofoil is still a challenging task. Evaluation of aerodynamic loads is especially complex in rotorcraft technology when the main or the tail rotor blades are concerned. Flow velocity components both along and perpendicular to a blade chord can vary in an arbitrary way as functions of time, due to the combined effects of rotor angular rotation, rotorcraft forward flight velocity, blade and/or hub elastic deformations and/or rotations in hub hinges. As a result, blade section angles of incidence can vary within a broad range including stall.

A need for simple and reliable methods for calculation of unsteady aerodynamic loads has increased lately, due to intensive investigations into the real time simulation and active control of aeroelastic structures. This is evident for instance in rotorcraft activity, where different concepts for "smart structures" and active control are explored [1,2]. An application of some additional control surfaces mounted on the blade is considered therein, which raises the problem of calculating unsteady aerodynamic loads on aerofoils with high lift devices like leading edge slots or trailing edge tabs [3].

The required properties of the method for calculation of aerodynamic loads stem both from the flow environment which is to be modelled and from prospective applications of the method.

Up till now in rotorcraft aeroservoelastic problems the assumption of a two dimensional flow environment has been justified. Within this assumption, the method should cover:

1. Three components of loads: lift, drag, and moment,
2. Arbitrary variations of: angle of attack, "horizontal" translation, (i.e. translation along the chord line or along the direction of undisturbed flow velocity), and "vertical" translation, (i.e. translation perpendicular to the chord line or to velocity of external flow),
3. Fluctuations of free stream velocity,
4. Shape of blade wakes,
5. Angle of incidence up to deep stall,

   and, which has became important recently,
6. Arbitrary trailing edge tab motion.

The method of calculation of aerodynamic loads should be compatible with existing computer codes for rotorcraft motion simulation and stability analysis. In helicopter rotor aeroelastic analysis ordinary differential equations are widely applied for calculating the steady and periodic motion of the rotor, Floquet or eigen-values for stability evaluation, and gains in control algorithms.

Some efficient methods developed in fluid dynamics for calculating unsteady loads are difficult to adopt in algorithms used for solving rotorcraft aeroelastic problems. For instance, application of panel methods leads to a large number of states. When some models are utilized the efficiency of numerical perturbation methods and algorithms for solving differential equation could be questioned.

The way to avoid some of the above mentioned difficulties is to express the flow motion in state variables, which allows the use of existing codes for aeroelastic analysis and the description of the changes of the loads or states by ordinary differential equations. These equations account for arbitrary aerofoil motion, and they also model the motion history, which is inherent in any unsteady aerodynamic loads case.

The classical approach for calculation of aerofoil unsteady loads in the frequency domain was developed first by Theodorsen [4]. The restrictions of his approach included the constant flow velocity, no chordwise aerofoil motion and the same motion of aerofoil and tab. Greenberg's [5] extension of this method concerned the varying free stream velocity, but not the tab. The extensions and modifications done by others [6-9] have not included a tab either.

The frequency domain formulation is suited mainly to searching for instability at one discrete frequency, which is not the case in rotary wing activity, where, due to periodic, parametric excitation, there is no definite frequency for instability. The need for a time domain approach is then evident.

The transformation to the time domain applied in [10] allows the release of the single frequency constraint in the above methods.

Arbitrary motion of an aerofoil with tab was investigated using indicial function concepts in [11], an extension of Greenbergs approach was developed in [12] and an heuristic application of the ONERA stall model was used in [13].

The objective of the research presented in this paper is to develop a method in the time domain for calculation of 2D aerodynamic loads on an aerofoil with trailing edge tab, both performing arbitrary motion, different for tab deflections and aerofoil translations. Unstalled flow is considered.

The method described in this study is considered to cover a more general case than in previous works, and is simpler and more computationally effective.

2. Formulation of the problem.

An inviscid, incompressible 2D flow with a free stream velocity U(t) which is an arbitrary function of time is assumed.

A thin, small cambered aerofoil with a trailing edge tab is considered. The aerofoil angle of incidence $\alpha(t)$ and the angle of tab deflection $\delta(t)$ are arbitrary functions of time not exceeding values at which flow separation occurs.

These assumptions allow the application of linear theory to small perturbations of flow velocity with the principle of superposition.

For the assumed flow, the perturbation φ of the velocity potential fulfils the Laplace equation

$$\nabla^2\varphi = 0 \tag{1}$$

The solution of equation (1) should satisfy the boundary conditions:

- at the aerofoil where the flow should be tangential to the surface, i.e. the flow velocity component perpendicular to the aerofoil matches that of the aerofoil

$$w(x,t) = W(x,t) \tag{2}$$

- at infinity where the perturbation of velocity potential should vanish.

Having calculated the velocity potential φ, the differential pressure on the aerofoil can be obtained from the linearized Bernoulli equation

$$\Delta p = -\rho \left[\frac{\partial}{\partial t} + U \frac{\partial}{\partial x}\right] \Delta\varphi \tag{3}$$

where $\Delta\varphi$ is the difference in the value φ between the upper and lower surface of the aerofoil

$$\Delta\varphi = \varphi|_U - \varphi|_L \tag{4}$$

Using the pressure distribution Δp, the lift and moment are calculated

$$L_o(t) = \int_{-b}^{b} (-\Delta p)\,dx, \qquad M_o(t) = -\int_{-b}^{b} (-\Delta p)\,x\,dx + abL(t) \tag{5}$$

It is assumed that lift is positive up. Moment is positive when aerofoil rotates the leading edge upward, and is calculated relative to the aerofoil aerodynamic centre situated at a distance ab from midchord.

The aerofoil force and moment are rearranged using the Bernoulli equation (3)

$$L_o(t)=\rho\int_{-b}^{b}\left[\frac{\partial\Delta\varphi}{\partial t}+U\frac{\partial\Delta\varphi}{\partial x}\right]dx, \qquad M_o(t)=-\rho\int_{-b}^{b}\left[\frac{\partial\Delta\varphi}{\partial t}+U\frac{\partial\Delta\varphi}{\partial x}\right]x\,dx+abL(t) \tag{6}$$

This is the "classical formulation" of aerofoil loads in two dimensional, unsteady flow.

3. The method of solution.

The approach proposed in this study consists of using the principle of superposition and calculating total unsteady loads as the sum of contributions from the aerofoil itself and tab:
- lift

$$L_o = L_\alpha + L_t \tag{7}$$

- moment

$$M_o = M_\alpha + M_t \tag{8}$$

- moment on the tab hinge

$$M_h = M_t \ (a=-1) \tag{9}$$

The same general expressions for calculating loads on the aerofoil and on the tab are derived. This result could have been achieved by appropriate adjustments in derivation of expressions for aerodynamic loads.

The method presented follows the classical approach to unsteady aerofoils [14]. First, the boundary conditions (2) on the aerofoil are expressed in terms of circulation. Next the integral equation is formulated which gives the relation between bound and shed circulation. The solution of this equation is calculated using decomposition of velocities and circulations into Fourier series [15].

In this method the coefficients of the Fourier series for an aerofoil and a tab are obtained separately.

Finally the expressions of unsteady loads are obtained in terms of velocities of aerofoil/tab motion and velocities induced by the wake by integrating the pressure distributions.

To calculate the loads effectively, assumptions concerning wake shape and its time dependence are necessary. For such a particular case, the transformation to the time domain is obtained via approximations of lift deficiency functions.

To check the validity of this method, the wake shape from [4] is considered and different approximations of lift deficiency function are analyzed to find the best one.

The loads calculated by this method are compared with other approaches and available experimental data.

4. Extension of unsteady thin aerofoil theory.

In this chapter the expressions of unsteady loads on aerofoil are re-derived and extended to account for arbitrary flow and aerofoil/tab motion.

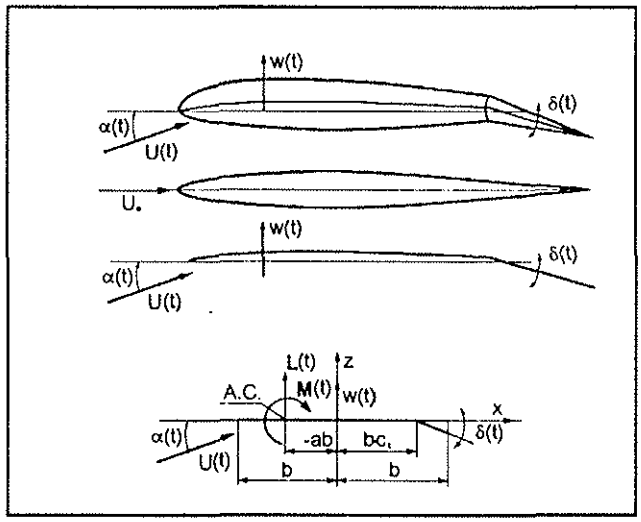

Fig.1.

Because of the small camber and thickness, the aerofoil is decomposed into two parts (Fig.1):

- a symmetrical profile, with the axis of symmetry along the mean flow velocity,
- a cambered mean line at incidence angle $\alpha(t)$ to the flow direction.

It is assumed here that the trailing edge tab influences aerodynamic loads in a similar way, as does changing of the aerofoil camber line.

For the symmetrical case the pressure distributions on the upper and lower surfaces of aerofoil are the same and there is no net force or moment.

For the unsymmetrical case the velocity potential and aerodynamic loads are decomposed into a circulatory part, which relates to the aerofoil/tab, and a noncirculatory part, which relates to the wake. At the trailing edge, these two parts are reconciled using the Kutta condition, which requires no discontinuity in velocity. The circulation γ_b results from the difference of velocity between the two points considered, so for x∈[-b, b]

$$\gamma_b = \Delta u = \frac{\partial \Delta\varphi}{\partial x} = \frac{\partial \varphi}{\partial x}\Big|_U - \frac{\partial \varphi}{\partial x}\Big|_L \tag{10}$$

because γ_b does not exist for x ∈ [-∞, -b]. From the definition of velocity potential, the difference $\Delta\varphi$ and its time derivative are expressed as

$$\Delta\varphi = \int_{\infty}^{x} \gamma_b \, dx = \int_{-b}^{x} \gamma_b \, dx, \qquad \frac{\partial \Delta\varphi}{\partial t} = \frac{\partial}{\partial t}\int_{-\infty}^{x} \gamma_b dx = \frac{\partial}{\partial t}\int_{-b}^{x} \gamma_b(x,t)\, dx \tag{11}$$

The flow velocity component in the boundary condition (2) is calculated as

$$W(x,t) = \frac{1}{2\pi}\int_{-b}^{\infty} \frac{\gamma(\zeta,t)}{x-\zeta} d\zeta \tag{12}$$

This expression is transformed into an integral equation [14] and inverted using Songen's kernel transformation

$$\gamma_b(x,t) = -\frac{2}{\pi}\sqrt{\frac{b-x}{b+x}}\int_{-b}^{b}\sqrt{\frac{b+\zeta}{b-\zeta}}\frac{W-\lambda}{x-\zeta} d\zeta \tag{15}$$

With a new spatial variable θ defined by

$$x = b\cos(\theta), \qquad x \subset [-b, b], \qquad \theta \subset [\pi, 0] \tag{16}$$

equation (15) is transformed to the form

$$\gamma_b = -\frac{2b}{\pi} tg\left(\frac{\theta}{2}\right)\int_{0}^{\pi}\frac{(1+\cos\vartheta)(W-\lambda)}{\cos\theta-\cos\vartheta} d\vartheta \tag{17}$$

The aerofoil/tab and wake velocities are decomposed in Fourier series

$$W = \sum_{n=0}^{\infty} W_n \cos(n\theta), \qquad \lambda = \sum_{n=0}^{\infty} \lambda_n \cos(n\theta) \tag{18}$$

After including (18) into (17), the circulation γ_b , which fulfils Kutta condition i.e. $\gamma_b=0$, is obtained in the form

$$\gamma_b=2\sum_{n=0}^{\infty}(w_n - \lambda_n)\, f_n(\theta), \quad f_0(\theta) = tg(\frac{\theta}{2}), \quad f_n(n\theta) = \sin(n\theta) \quad for\ n\geq 1 \tag{19}$$

The coefficients of the series of the induced velocity λ due to wake circulation are calculated as

$$\lambda_n = \frac{2}{\pi}\int_b^{\infty}\lambda\cos(n\theta)d\theta = -\frac{1}{\pi}\int_b^{\infty}\gamma_w(t,\zeta)\frac{[\zeta-\sqrt{\zeta^2-b^2}]^n}{b^n\sqrt{\zeta^2-b^2}}d\zeta \tag{20}$$

Using the series (19), lift and moment are expressed as

$$L(t) = -\,2\pi\rho bU[(w_0+\frac{1}{2}w_1)-(\lambda_0+\frac{1}{2}\lambda_1)] + \rho\,\pi b^2\frac{\partial}{\partial t}[(w_0-\frac{1}{2}w_2)-(\lambda_0-\frac{1}{2}\lambda_2)] \tag{21}$$

$$\begin{aligned} M(t) = &-\frac{\pi}{2}\rho b^2U[(w_1+w_2)-(\lambda_1+\lambda_2)] + (\frac{1}{2}+a)bL(t) \\ &-\frac{\rho\pi b^2}{8}\frac{\partial}{\partial t}[(w_1-w_3)+4(w_0-\frac{1}{2}w_2)-(\lambda_1-\lambda_3)-4(\lambda_0-\frac{1}{2}\lambda_2)] \end{aligned} \tag{22}$$

Conservation of circulation gives the relation

$$2\pi b(w_0+\frac{1}{2}w_1) = -\int_b^{\infty}\gamma_w(t,\zeta)\sqrt{\frac{\zeta+b}{\zeta-b}}d\zeta \tag{23}$$

Inserting (20) into (21) and (22) and then using (23) and rearranging, the lift is obtained in a "standard unsteady aerodynamics" form

$$\begin{aligned} L(t) = &\pi\rho b^2(\dot{w}_0-\frac{1}{2}\dot{w}_2) + \\ &+2\pi\rho bQ(t)\left\{1-\int_b^{\infty}\gamma_w(\sqrt{\frac{\zeta+b}{\zeta-b}}-1)d\zeta+\frac{1}{U}\frac{\partial}{\partial t}\int_b^{\infty}\gamma_w(\zeta-\sqrt{\zeta^2-b^2})d\zeta\right\}\left\{\int_b^{\infty}\gamma_w\sqrt{\frac{\zeta+b}{\zeta-b}}\right\}^{-1} \end{aligned} \tag{24}$$

where

$$Q(t) = U(t)(w_0+\frac{1}{2}w_1) \tag{25}$$

and the expression

$$C_l(\gamma_w,t) = \left\{1-\int_b^\infty \gamma_w\left(\sqrt{\frac{\zeta+b}{\zeta-b}}-1\right)d\zeta+\frac{1}{U}\frac{\partial}{\partial t}\int_b^\infty \gamma_w(\zeta-\sqrt{\zeta^2-b^2})d\zeta\right\}\left\{\int_b^\infty \gamma_w\sqrt{\frac{\zeta+b}{\zeta-b}}\right\}^{-1} \tag{26}$$

is a lift deficiency function in the time domain.

The influence of the wake on moment comes from the lift contribution and from the wake itself. The wake influence is expressed as

$$\begin{aligned} C_m(\gamma_w,t) &= \int_b^\infty \gamma_w[\zeta-\sqrt{\zeta^2-b^2}]\left[\sqrt{\frac{\zeta+b}{\zeta-b}}-1\right]d\zeta+ \\ &+\frac{\rho}{4}\frac{\partial}{\partial t}\left\{\int_b^\infty \gamma_w[\zeta-\sqrt{\zeta^2-b^2}]^2 d\zeta+2b\int_b^\infty \gamma_w[\zeta-\sqrt{\zeta^2-b^2}]d\zeta\right\} \end{aligned} \tag{27}$$

The aerodynamic loads are decomposed into noncirculatory and circulatory parts

$$L(t) = L_N(t) + L_C(t) \tag{28}$$

$$L_N(t) = \pi\rho b^2(\dot{w}_0-\frac{1}{2}\dot{w}_2), \quad L_C(t)=2\pi\rho Q(t)C_l(\gamma_w,t) \tag{29}$$

$$M(t) = M_N(t) + M_C(t) \tag{30}$$

$$\begin{aligned} M_N(t) &= -\frac{\pi\rho b^2}{8}[4U(w_1+w_2)-b(\dot{w}_0-\dot{w}_3)-4b(\dot{w}_0-\frac{1}{2}\dot{w}_2)]+(\frac{1}{2}+a)bL_N(t) \\ M_C(t) &= -\frac{1}{2}\rho UC_m(\gamma_w,t)+(\frac{1}{2}+a)bL_C(t) \end{aligned} \tag{31}$$

To obtain effective expressions for calculating lift and moment, the dependence of velocities and circulations on time and on spatial coordinates should be established.

The above derived expressions are valid for loads on the aerofoil and the tab with the proper adjustments of tab velocities given in the next section.

5. Modifications for tab loads.

The tab rotation relative to the aerofoil changes the direction of the free stream velocity and gives its own contribution to the flow velocity

$$w_{t0} = U(t)\delta(t)-bc_\beta\dot{\delta}(t) \qquad w_{t1} = b\dot{\delta}(t) \tag{32}$$

To obtain formulae for the Fourier series (19) for the tab only the first two harmonics of the spatial function for tab velocity are taken into account. The bound circulation of the tab is first calculated in the form

$$\gamma_{bT} = \frac{2}{\pi}\sum_{n=0}^{\infty} f_{Tn}(\theta) \tag{33}$$

where

$$\begin{aligned}
f_{T0}(\theta) &= tg(\frac{\theta}{2})[\phi_0(w_{t0}-\lambda_{t0})+(w_{t1}-\lambda_{t1})\sin\phi_0)\\
f_{T1}(\theta) &= \sin(\theta)\left\{2(w_{t0}-\lambda_{t0})\sin\phi_0+(w_{t1}-\lambda_{t1})[\phi_0+\frac{\sin(2\phi_0)}{2}]\right\}\\
f_{t2}(\theta) &= \sin(2\theta)[(w_{t0}-\lambda_{t0})\sin(2\phi_0)+\frac{2}{3}(w_{t1}-\lambda_{t1})(\sin2\phi_0\cos\phi_0+\sin\phi_0)]\\
f_{t3}(\theta) &= \sin(3\theta)[(\frac{2}{3})(w_{t0}-\lambda_{t0})\sin(3\phi_0)+(w_{t1}-\lambda_{t1})\frac{\sin(2\phi_0)}{2}]
\end{aligned} \tag{34}$$

and the rest of series

$$R = \sum_{n=4}^{\infty}(\frac{1}{n})\sin(n\phi_0)\{2\sin(n\theta)(w_{t0}-\lambda_0)+[\sin((n+1)\theta)+\sin((n-1)\theta)]w_{t1}\} \tag{35}$$

In the above formulae the value of Φ_0 relates to the tab x coordinate.

The main difficulty in obtaining (33) lies in the calculation of the Glauert integral

$$I_n = \int_0^{\Phi_0}\frac{\cos(n\vartheta)}{\cos(\vartheta)-\cos(\theta)}d\vartheta \tag{36}$$

for the boundaries appropriate to tab coordinates. This is solved by decomposing the integrand into series.

After rearranging (34) to the same form as (19) one obtains for the tab

$$\begin{aligned}
w_{T0} &= \phi_0 w_{t0}+w_{t1}\sin\phi_0 \qquad w_{T1} = 2w_{t0}\sin\phi_0+w_{t1}(\phi_0+\frac{\sin(2\phi_0)}{2})\\
w_{T2} &= w_{t0}\sin(2\phi_0)+\frac{2}{3}(w_{t1}(\sin2\phi_0\cos\phi_0+\sin\phi_0),\\
w_{T3} &= (\frac{2}{3})w_{t0}\sin(3\phi_0)+w_{t1}\frac{\sin(2\phi_0)}{2}
\end{aligned} \tag{37}$$

6. Classic unsteady aerofoil case.

In the following the assumptions for the wake from [4] are applied. The wake shape is not spatially dependent and flow disturbance is convected downstream with a mean flow velocity, so

$$\frac{\partial \gamma_w}{\partial \zeta} = 0, \qquad \zeta = \zeta(t) = b + U(t)t, \qquad \frac{\partial \zeta}{\partial t} = U(t) \tag{38}$$

In this case the lift deficiency function $C_f(\gamma,k)$ has the form

$$C(\gamma_w,t) = C(\gamma_w,t)_f = \{\int_b^\infty \gamma_w(t,\zeta)\frac{\zeta}{\sqrt{\zeta^2-b^2}}d\zeta\}\{\int_b^\infty \gamma_w(t,\zeta)\sqrt{\frac{\zeta+b}{\zeta-b}}d\zeta\}^{-1} \tag{39}$$

The same assumptions results in the influence of the wake on the moment being zero.

For the case considered the lift and moment are written in the form

$$\begin{aligned} L(t) &= 2\pi\rho b Q(t)\ C(t,\gamma_w) + \pi\rho b^2(\dot{w}_0 - \frac{1}{2}\dot{w}_2) \\ M(t) &= -\frac{\pi}{2}\rho b^2 U(t)(w_1+w_2) - \frac{\pi\rho b^3}{8}(\dot{w}_1-\dot{w}_3) - \frac{\pi\rho b^3}{2}(\dot{w}_0-\frac{1}{2}\dot{w}_2) + (\frac{1}{2}+a)bL(t) \end{aligned} \tag{40}$$

or as coefficients

$$\begin{aligned} C_{L_N}(t) &= \frac{\pi b}{U_0^2}(\dot{w}_0-\frac{1}{2}\dot{w}_2), \qquad C_{L_C}(t) = \frac{2\pi}{U_0^2}Q(t)C(\gamma_w,t) \\ C_{M_N}(t) &= -\frac{\pi b}{U_0^2}\left[U(t)(w_1+w_2) - \frac{b}{8}(\dot{w}_1-\dot{w}_3) - \frac{b}{2}(\dot{w}_0-\frac{1}{2}\dot{w}_2)\right] + (\frac{1}{2}+a)C_{L_N}(t), \\ C_{M_C}(t) &= (\frac{1}{2}+a)C_{L_C}(t) \end{aligned} \tag{41}$$

This is the generalization of classical unsteady theory to arbitrary aerofoil/tab motion. To obtain the loads, usually the harmonic motion is assumed and a Laplace transformation utilized to calculate the function $C(\gamma_w,t)$ in frequency domain. This part of derivation is not included here.

7. Transformation to time domain.

Having the lift deficiency function in the frequency domain, and assuming that the motion does not differ much from periodic, the calculation of airloads can be transferred to the time domain. According to (40) only the circulatory part of the lift is considered.

Applying a Laplace transformation to both sides of the second equation in (29) one obtains

$$\mathcal{L}\{L_C(t)\} = 2\pi\rho b\mathcal{L}\{Q(t)\}\mathcal{L}\{C(t)\} \tag{42}$$

or

$$L_C(s) = 2\pi\rho bQ(s)C(s) \tag{43}$$

where $L_C(s)$, Q(s) and C(s) are Laplace transforms of $L_C(t)$, Q(t) and C(t).

Function C(s) is put in the form

$$C(s) = \frac{H(s)}{K(s)} \tag{44}$$

and a new state variable X(s) is defined as

$$X(s)K(s) = Q(s) \tag{45}$$

Including (44) and (45) in (43) and applying the inverse Laplace transform, the circulatory lift in time domain is obtained

$$L_C(t) = 2\pi\rho b\mathcal{L}^{-1}\{H(s)X(s)\} \tag{46}$$

Usually, because of the complex form of function C(s), it is difficult to find the inverse transformation, even for the simple wake pattern assumed here. The expression (44) is then used to approximate the lift deficiency function with H(s) and K(s) assumed as two polynomials of the M-th order

$$H(s) = \sum_{m=0}^{M} a_m s^m; \quad K(s) = \sum_{m=0}^{M} b_m s^m \tag{47}$$

Coefficients of these polynomials are determined by the proper approximation of function C(s) in the frequency domain.

The right hand side of (45) is transformed to the form

$$X(s)[b_0 + s^M + \sum_{m=1}^{M-1} b_m s^m] = Q(s) \tag{48}$$

Applying an inverse Laplace transformation to both sides of this equation yields

$$\frac{d^M}{dt^M}X(t) + \sum_{m=1}^{M-1} b_m \frac{d^m}{dt^m}X(t) + b_0 X(t) = Q(t) \tag{49}$$

Having solved equation (49), the circulatory component of the lift is calculated as

$$L_C(t) = 2\pi\rho b\left[(a_0 - a_M b_0)X(t) + \sum_{m=1}^{M-1}(a_m - a_M b_m)Y_m(t) + a_M Q(t)\right] \tag{50}$$

where

$$Y_m = \frac{d^m X}{dt^m} \tag{51}$$

The results of calculations based on the present method are discussed in the following chapters.

8. Verification of the method.

To verify the method, first the different approximations of lift deficiency function are investigated. Next the unsteady loads calculated in the time domain are compared with results obtained by other authors and experiments. Finally the loads for the aerofoil and tab performing different motions are presented.

8.1. Approximations of Theodorsen function.

The lift deficiency function derived in [4] has the form

$$C(k) = \frac{H_1^{(2)}(k)}{H_1^{(2)}(k) + i\,H_0^{(2)}(k)}$$

The approximations considered here have the form

$$C(s) = \frac{\sum_{m=1}^{m=M} a_m s^m + a_0}{s^M + \sum_{m=M-1}^{1} b_m s^m + a_0}$$

The coefficients of approximating polynomials up to the third order are given in the following table:

	a_3	a_2	a_1	a_0	b_1	b_2
I [16]			0.55	0.15		
II		0.5	0.28076	0.01365	0.3455	
III [17]	0.50465	0.4414	0.07566	0.00189	0.08512	0.64750

For these approximations the real and imaginary parts of the lift deficiency function are compared in Fig.2.

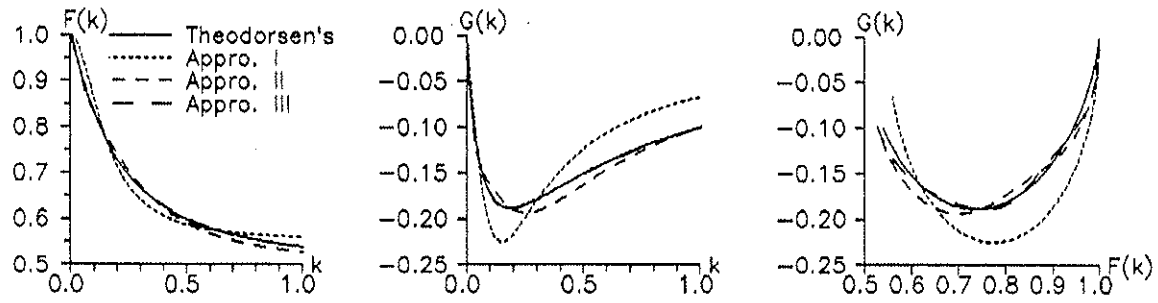

Fig.2. Comparison of original and approximated lift deficiency functions.

The second and third order approximation gives fairly good agreement with the original function, especially for the lower reduced frequency range.

8.2. Aerofoil loads.

In this section an aerofoil without a tab is considered.

To check the validity of approximations and the transformation to the time domain, the amplitude and phase of lift obtained from the third order approximation and original function is shown in Fig.3 for pitch motion and in Fig.4 for plunge motion. The curves calculated are practically undistinguishable from those obtained using Theodorsens function. This confirms the feasibility of this approach.

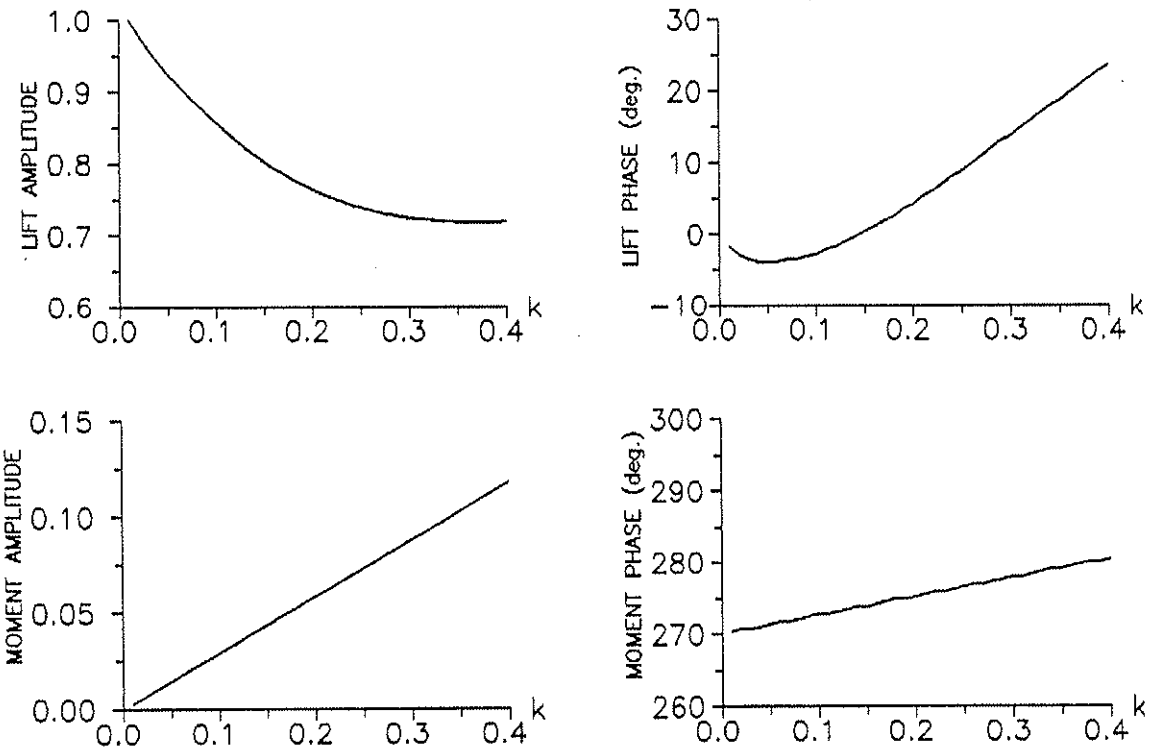

Fig.3. Calculated amplitude and phase for lift and moment on aerofoil.
Pitch motion. Third order approximation of Theodorsen function.

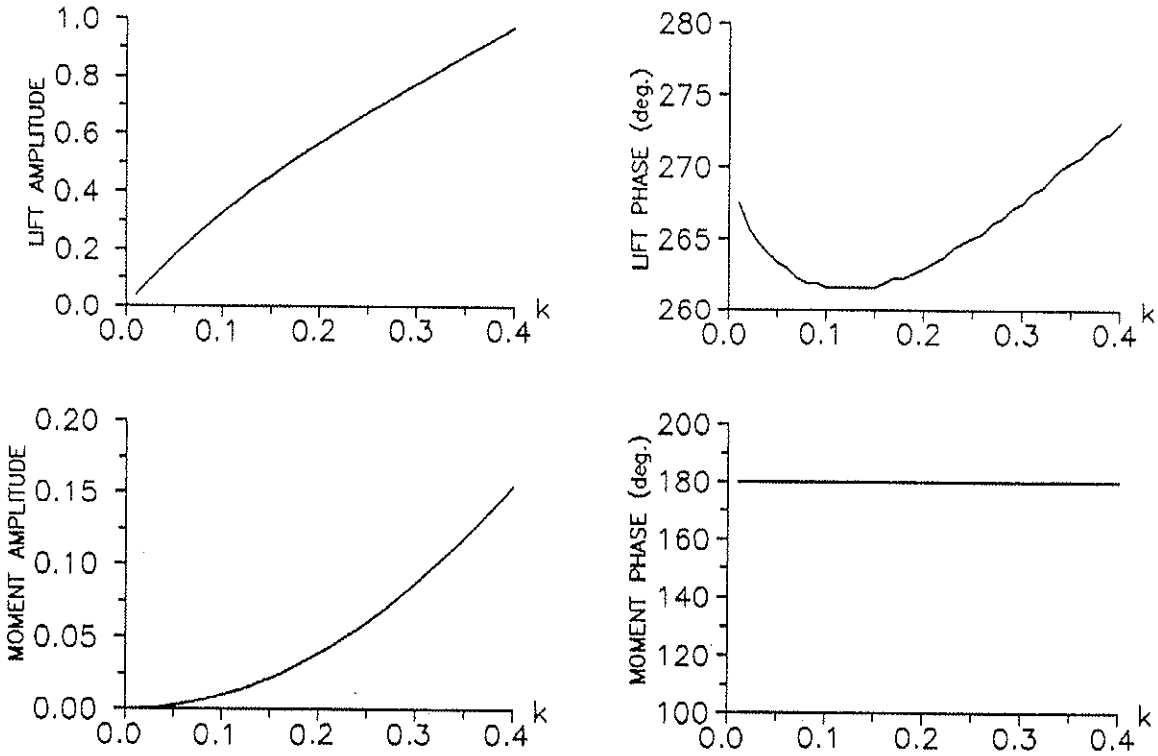

Fig.4. Calculated amplitude and phase for lift and moment on aerofoil.
Plunge motion. Third order approximation of Theodorsen function.

Lift and moment calculated for aerofoil motion are compared with the experimental data for NACA 23010 aerofoil [18] for pitch motion in Fig.5 and for plunge motion in Fig.6.

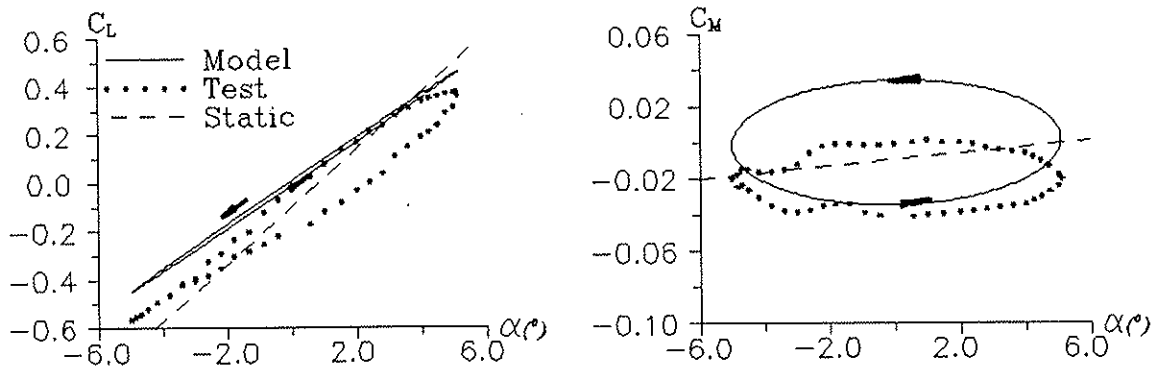

Fig.5. Comparison of calculated lift and moment with experimental data for NACA 23010 aerofoil.
Pitch motion, k=0.125, Ma=0.4. Third order approximation of Theodorsen function.

In both cases lift hysteresis is less intensive for the calculated results. The lift curve slope of the calculated results is the same as that obtained from experiment data for the pitch case and differs slightly for the pure plunge case. This suggests, that the lift deficiency function for plunge motion should be slightly different, than for aerofoil pitch. Taking into

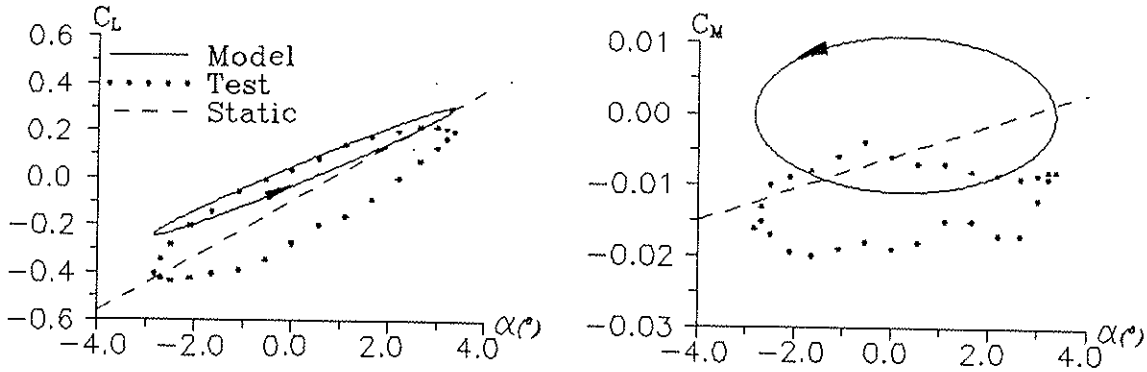

Fig.6. Comparison of calculated lift and moment with experimental data for NACA 23010 aerofoil. Plunge motion, k=0.129, Ma=0.4. Third order approximation of Theodorsen function.

account that in the calculations the lift curve slope is taken as 2π, the agreement with experiment is fairly good.

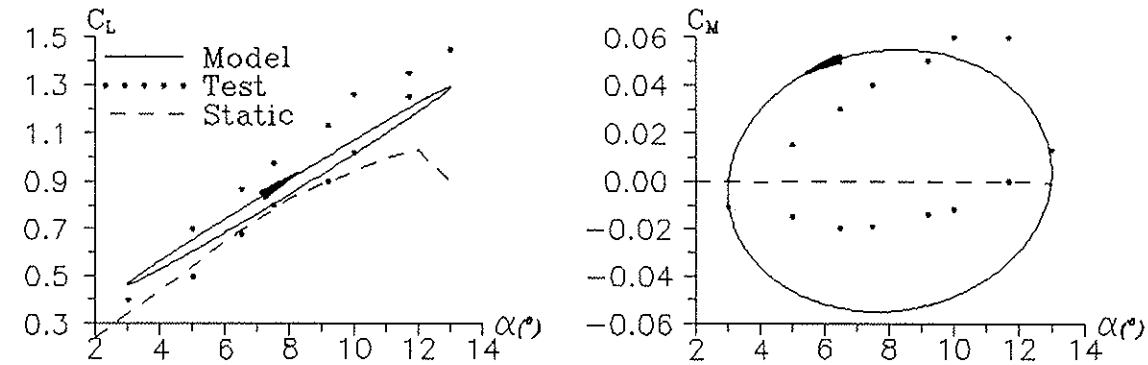

Fig.7. Comparison of calculated lift and moment with experimental data for NACA 0012 aerofoil. Plunge motion, k=0.2, Ma=0.3. Third order approximation of Theodorsen function.

A similar comparison for the NACA 0012 aerofoil with the results presented in [19] is shown in Fig.7.

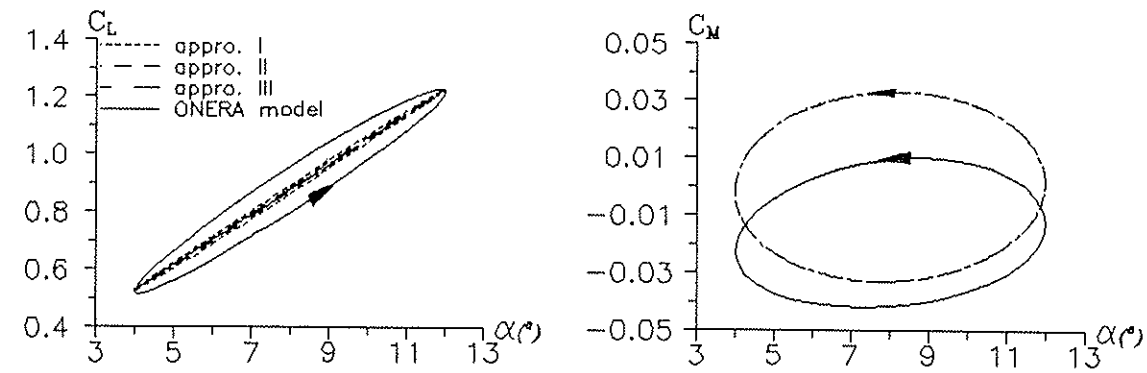

Fig.8. Comparison with ONERA model for different approximations of lift deficiency function. Pitch motion, k=0.15.

In Fig.8 the comparison of lift and moment with results from the ONERA model modified in [13] is shown for all three aproximations of the lift deficiency function. The second and third order approximation of lift deficiency function gives the most intensive hysteresis.

8.3. Aerofoil with tab.

There are few experimental data relating to aerofoils with tabs, which can be used for comparison purposes. Considerable experimental evaluation performed by the NLR concerns mainly higher Mach numbers and frequencies.

In Fig.9. the effects of the influence of reduced frequency for an aerofoil with deflecting tab is presented as functions of angle of attack and time. The trend shown is in good agreement with [18].

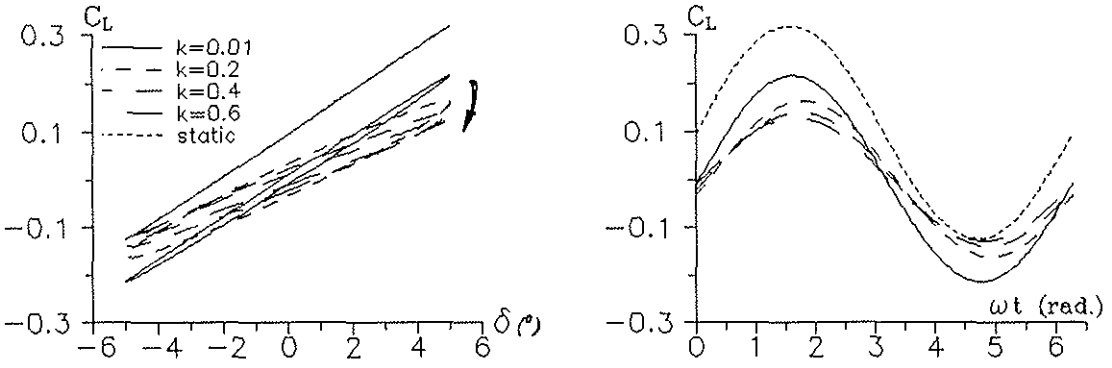

Fig.9. Calculated lift on fixed aerofoil with oscilating tab for different reduced frequencies.

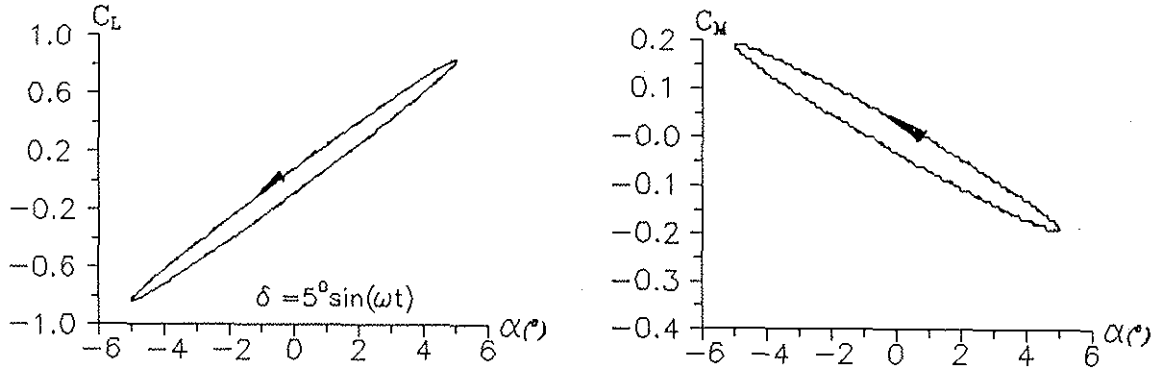

Fig.10. Calculated loads on aerofoil with tab oscillating with the same frequencies.

The results of calculations for Theodorsen's case, i.e. an aerofoil with tab oscillating with the same frequencies, are shown in Fig.10. The results are exactly the same as those obtained from the original expressions [4].

In Fig.11 the results of calculations according to the present theory and the modified ONERA model [13] are compared. The aerofoil is performing pitch oscillations and the tab deflection amplitude is ±10°. For the lower aerofoil and tab frequency ratios, both methods predict qualitatively the same load changes. At higher aerofoil and tab frequency ratios, the present model gives the more reliable results, as the changes of aerofoil loads are more in accord with the ratio of aerofoil/tab frequencies.

The tab motion changes the amount of energy involved in the aerofoil motion, which manifests itself by the differently shaped hysteresis loops. This could influence the blade aeroelastic behaviour and possibly lead to a tab induced type of blade instability.

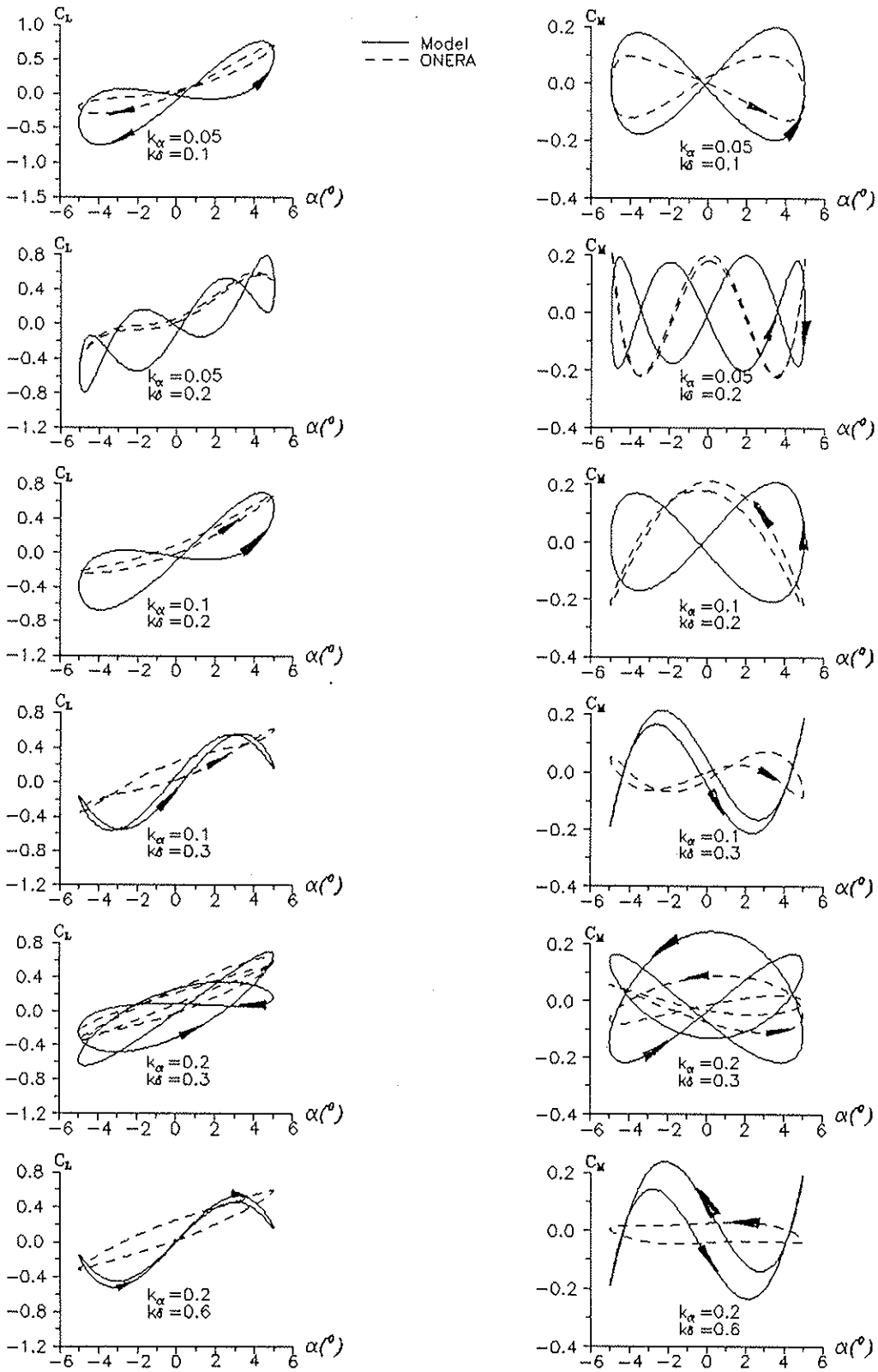

Fig.11. Comparison of calculated aerofoil loads with modified ONERA model for pitching aerofoil and oscillating tab. Amplitude of tab motion ±10°.

Conclusions.

The 2D aerofoil theory for incompressible, inviscid flow is extended to the case of aribtrary aerofoil/tab motion and varying free stream velocity. The expressions for calculating lift and moment have general form and are valid for arbitrary wake shape. The obtained formulae are easily programmed, as the same expressions are valid for aerofoil and tab the only difference being in the velocity expressions involved.

The theory is validated using the classical Theodorsen case and compared with experimental data. For this case the transformation to the time domain is performed using a Laplace transformation for approximation of the lift deficiency function.

The influence of mutually different aerofoil and tab frequencies on aerodynamic loads is presented.

Acnowledgments.

The present work forms a part of a research project funded by UK EPSRC on "Application of Smart Structures to Helicopter Rotor Blade Design". The support of the Government of the Peoples' Republic of China for the second author is also acknowledged.

Bibliography

1. Narkiewicz J., Done G.T.S., "An Overview of Smart Structure Concepts for the Control of Helicopter Rotor", Second European Conference on Smart Structures and Materials, Glasgow, October 1991.
2. Friedmann P.P., "Rotary-Wing Aeroservoelastic Problems", Proceedings of European Conference on Aeroelasticity, 1991.
3. Yu Y.H., Lee S., McAlister K.W., Tung Ch., Wanng C.M., "High Lift Concepts for Rotorcraft Application", 49th American Helicopter Society Forum, St.Louis, Mo, May 1993.
4. Theodorsen T., "General Theory of Aerodynamic Instability and the Mechanism of Flutter", NACA Rep. No.496, 1935.
5. Greenberg K.M.,"Airfoil in Sinusoidal Motion in a Pulsating Stream", NACA Rep. No.1326, 1947.
6. Loewy R.G., "A Two-Dimensional Approximation to the Unsteady Aerodynamics of Rotary Wings", Journal of the Aeronautical Sciences, Vol.24, No.2, February 1957.
7. Kottapalli S.B.R.,"Unsteady Aerodynamics of Oscillating Airfoils with Inplane Motion", Journal of the American Helicopter Society, Vol. 30, No. 1, 1985.
8. Kaza K.R.V., Kvaternik R.G., "Application of Unsteady Airfoil Theory to Rotary Wings", Journal of Aircraft, Vol.18, No.7, 1981.
9. Johnson W., "Application of Unsteady Airfoil Theory to Rotary Wings", Journal of Aircraft, Vol.17, No.4, 1980.
10. Dinyavari M.A.H., Friedmann P.P.:"Application of Time-Domain Unsteady Aerodynamics to Rotary Wing Aeroelasticity", AIAA Journal, Vol.24, No.9, September 1986.
11. Leishman J.G.:"Unsteady Lift of an Airfoil with a Trailing Edge Flap based on Indicial Concept", Pap. No.19, Eighteenth European Rotorcraft Forum, Avignon, France, September 1992.
12. Millot T., Friedmann P.P.,"Vibration Reduction in Helicopter Rotors Using an Active Control Surface Located on the Blade", 33rd AIAA Struct., Str. Dyn. and Mat. Conf., Dallas, Texas, April, 1992.
13. Narkiewicz J., Rogusz M., "Smart Flap for Helicopter Rotor Blade Performance Improvement", XIX European Rotorcraft Forum, Cernobbio (Como), Italy, September 1993.
14. Dowell E.H., Curtiss H.C.jr, Scanlan R.M., Sisto F.,"A Modern Course in Aeroelasticity", Sijthoff Nordhoff, The Netherlands, 1979.
15. Johnson W., "Helicopter theory",Princeton University Press, 1980
16. Spangler R.L. Jr, Hall S.R.,"Piezoelectric Actuators for Helicopter Rotor Control", 31st AIAA Struct., Str. Dyn. and Mat. Conference, Long Beach, CA, April 2-4, 1990.
17. Van der Vooren, "Collected Tables and Graphs", AGARD Manual on Aeroelsticity, Vol.VI, Part VI, January 1964.
18.Tyler J.C., Leishman J.G., "Analysis of Pitch and Plunge Effects on Unsteady Airfoil Behavior", 47th American Helicopter Society Forum, Phoenix, Az, May 1991.
19. He Ch.J., Du Val R., "An Unsteady Airload Model with Dynamic Stall for Rotorcraft Simulation", 50th American Helicopter Society Forum, Washington D.C., May 1994.